Causes and consequences of resource heterogeneity in forests: interspecific variation in light transmission by canopy trees

CHARLES D. CANHAM[1]
Institute of Ecosystem Studies, Millbrook, NY 12545, U.S.A.
ADRIEN C. FINZI AND STEPHEN W. PACALA[2]
Ecology and Evolutionary Biology, The University of Connecticut, Storrs, CT 06268, U.S.A.
AND
DIANE H. BURBANK[3]
Institute of Ecosystem Studies, Millbrook, NY 12545, U.S.A.

Received February 23, 1993
Accepted August 10, 1993

CANHAM, C.D., FINZI, A.C., PACALA, S.W., and BURBANK, D.H. 1994. Causes and consequences of resource heterogeneity in forests: interspecific variation in light transmission by canopy trees. Can. J. For. Res. **24**: 337–349.

We have analyzed the light transmission characteristics of the nine deciduous and coniferous species that dominate the transition oak – northern hardwood forests of southern New England. Maximum likelihood techniques were used to estimate species-specific light extinction coefficients, using fish-eye photography combined with data on the locations and geometry of trees in the neighborhood around each photo point. Quantum sensors were also used to quantify interspecific variation in the importance of sunflecks and beam enrichment. Variation in light extinction was closely correlated with shade tolerance and successional status of the species. The most shade-tolerant species (*Fagus grandifolia* Ehrh. and *Tsuga canadensis* (L.) Carr.) cast the deepest shade (<2% of full sun), while earlier successional species such as *Quercus rubra* L. and *Fraxinus americana* L. allowed greater light penetration (>5% full sun). These differences were more closely related to differences in crown depth than to differences in light extinction per unit depth of crown. Sunflecks contributed relatively little radiation beneath late successional species (<10% of total understory photosynthetically active radiation), but represented a major fraction (40–50%) of radiation beneath less shade-tolerant species. Using growth and mortality functions for the same species developed in a related study, our results indicate that saplings of all of the species have high survivorship in the shade cast by conspecific adults. However, only the three most shade-tolerant species have low rates of sapling mortality under the low light levels characteristic of stands dominated by late successional species. Our results are consistent with previously reported models, which propose that secondary succession is driven by interspecific differences in resource uptake and tolerance.

CANHAM, C.D., FINZI, A.C., PACALA, S.W., et BURBANK, D.H. 1994. Causes and consequences of resource heterogeneity in forests: interspecific variation in light transmission by canopy trees. Can. J. For. Res. **24** : 337–349.

Nous avons analysé les caractéristiques de la transmission de la lumière de neuf espèces feuillues et coniférienes qui dominent les forêts transitionnelles de chêne et feuillus nordiques du sud de la Nouvelle-Angleterre. Les techniques de vraisemblance maximale furent utilisées pour estimer les coefficients d'extinction lumineuse de chaque espèce, en faisant appel à la photographie grand-angulaire combinée aux données de localisation et de géométrie des arbres aux alentours de chaque échantillon photographique. Des senseurs de quanta ont aussi été utilisés pour évaluer la variation interspécifique dans l'importance des taches de lumière et de l'enrichissement du rayonnement direct. La variation de l'extinction lumineuse a montré une forte corrélation à la tolérance à l'ombre et au statut successionnel des espèces. Les espèces les plus tolérantes à l'ombre (*Fagus grandifolia* Ehrh. et *Tsuga canadensis* (L.) Carr.) produisent l'ombrage la plus dense (<2% du rayonnement de plein jour), tandis que les espèces pionnières comme *Quercus rubra* L. et *Fraxinus americana* L. laissent pénétrer plus la lumière (>5% du rayonnement de plein jour). Ces différences sont davantage liées aux différences dans la longueur de la cime qu'à celles de l'extinction lumineuse par unité de longueur de cime. Les taches de lumière fournissent relativement peu de rayonnement sous les espèces successionnelles tardives (<10% de la radiation utile pour la photosynthèse total sous couvert), mais fournissent une partie importante du rayonnement (40–50%) sous les espèces moins tolérantes à l'ombre. Grâce aux fonctions de croissance et de mortalité conçues pour les mêmes espèces dans une étude conjointe nos résultats indiquent que les semis de toutes les espèces ont une survie élevée dans l'ombre des adultes de leur propre espèce. Cependant, seules les trois espèces les plus tolérantes ont de faibles taux de mortalité sous la basse intensité lumineuse caractéristique des stations dominées par les espèces successionnelles tardives. Nos résultats sont cohérents avec d'autres modèles qui proposent que la succession secondaire soit engendrée par des différences interspécifiques dans l'utilisation des ressources et la tolérance.

[Traduit par la rédaction]

---

[1]Author to whom all correspondence should be addressed.
[2]Present address: Ecology and Evolutionary Biology, Princeton University, Princeton, NJ 08544, U.S.A.
[3]Present address: Green Mountain and Finger Lakes National Forest, Rutland, VT 05702, U.S.A.

Printed in Canada / Imprimé au Canada

Introduction

It has become almost axiomatic among forest ecologists that treefall gaps create spatial heterogeneity in understory light levels (March and Skeen 1976; Chazdon and Fetcher 1984; Canham 1988; Canham et al. 1990), and that this spatial heterogeneity is necessary for the maintenance of species diversity in old-growth forests (Denslow 1980, 1985, 1987; Runkle 1981). In the absence of discrete gaps, more modest levels of heterogeneity in understory light regimes are created by processes such as physical damage to leaves and branches, herbivory, and disease (Clark and Clark 1991), and by diurnal and seasonal changes in sun angles (Rich et al. 1993). While physiological responses to fine-scale temporal and spatial variation created by sunflecks have been widely studied (Pearcy 1983, 1987; Chazdon 1988), the community-level effects of resource heterogeneity beneath intact canopies have received relatively little attention. The often-drawn dichotomy between resource-rich gaps and a surrounding matrix of spatially uniform, resource-poor understory may reflect the fact that most studies of gap-phase dynamics have focused on old-growth forests (see reviews in Brokaw 1985; Runkle 1985), where the canopy is dominated by shade-tolerant tree species that cast deep shade, and where treefall disturbance is the predominant cause of spatial heterogeneity in understory light levels (Canham et al. 1990).

While canopy disturbances can still create resource heterogeneity in successional stands, the linkage between small-scale disturbance and either species diversity or canopy dynamics is clearly much weaker than in old-growth stands. In contrast with the acknowledged importance of abiotic disturbance as a cause of resource heterogeneity in old-growth forests, we present here results that document the importance of a biotic process as a major cause of heterogeneity in understory light levels in both successional and old-growth stands. We specifically focus on interspecific variation in light transmission by canopy trees, and consider the importance of these interspecific differences for the dynamics of secondary succession.

Horn's (1971) monograph on the adaptive geometry of trees remains one of the few studies to link interspecific variation in light transmission by canopy trees with predictions of the outcome of secondary succession in forests. Horn (1971) demonstrated that canopy openness was inversely correlated with shade tolerance among tree species. Horn (1971, 1974, 1975, 1976), and later Connell and Slatyer (1977) suggested that these interspecific differences in resource depletion and tolerance provided the basis for a general model of secondary succession in forests (i.e., Connell and Slatyer's "tolerance" model). Despite the potential importance of these interspecific differences in light transmission, there has been very little follow-up to Horn's early research.

Competition for light in forests is clearly a neighborhood phenomenon (sensu Pacala and Silander 1985); shading by neighboring trees largely determines local light availability in a forest understory. Analyses of neighborhood competition for soil resources usually have been based on analyses of the responses of target plants to the abundance of neighbors (e.g., Pacala and Silander 1985, 1990; Silander and Pacala 1985; Goldberg 1987). However, it is clear that the effects of neighboring canopy trees (or the absence of trees in canopy gaps) are spatially explicit; incident radiation is highly directional, and the effect of a tree (or a gap) will depend on its position, geometry, and light transmission characteristics. While many studies have made the simplifying assumption that light flux through forest canopies is predominantly a vertical process (e.g., Horn 1971), it is clear that the geometry of light transmission has a profound effect on forest dynamics (Canham 1988; Canham et al. 1990). For example, the dynamics of canopy recruitment by sugar maple (*Acer saccharum* Marsh.) and beech (*Fagus grandifolia* Ehrh.) depend strongly on the penetration of light through gaps into the understory beneath the northern edges of gaps (Canham 1985, 1990).

The study of light transmission through plant canopies has been dominated by theoretical models that offer a great deal of analytical detail on the spatial and temporal dynamics of the supply and depletion of light (e.g., Ross 1981). While a number of these models have been parameterized for agronomic crops (e.g., Norman 1979), there are very few examples of empirically based models of light transmission for the much more structurally complex case of a multispecies forest (e.g., Wang and Baldocchi 1989). Physiologically based models of whole-canopy carbon gain often employ highly detailed assumptions about canopy structure and light transmission; however, they are generally limited to short (≤1 year) time scales because of the large number of parameters required (Norman and Jarvis 1975; Grace 1990). Models for the dynamics of multispecies forests over longer time scales, such as the widely studied class of JABOWA and FORET stand simulation models (Botkin et al. 1972; Shugart 1984), use simplified submodels for light extinction, usually based on some form of a nonspatial Beer's Law (Shugart 1984).

The research reported here quantifies interspecific differences in the transmission of photosynthetically active radiation (PAR) by the deciduous and coniferous species that dominate the transition oak – northern hardwood forests of southern New England. The nine species chosen for study (listed in order of decreasing shade tolerance in these forests, as indicated by ability of saplings to survive under low light (Pacala et al. 1993)) were beech, eastern hemlock (*Tsuga canadensis* (L.) Carr.), sugar maple, yellow birch (*Betula lutea* Michx.), black cherry (*Prunus serotina* Ehrh.), white pine (*Pinus strobus* L.), red maple (*Acer rubrum* L.), white ash (*Fraxinus americana* L.), and northern red oak (*Quercus rubra* L.). The research was designed to provide parameter estimates for a spatially explicit model of light transmission through stands containing this diverse mix of species. The light transmission model serves as a key submodel for a new, empirically based, spatially explicit model of forest dynamics (SORTIE, described in Pacala et al. 1993).

Methods

Study area

Our research was conducted in and around the Great Mountain Forest of northwestern Connecticut (42°N, 73°15′W). The forest is located on Canaan Mountain, at elevations of 350–550 m. Forests in this region are dominated by representatives of both the conifer–hardwood forests of northern New England and the oak forests of southern New England. The nine species selected for study included all of the dominant and the major subordinate species of both mid- and late-successional forests. All of the sites used in our study were second-growth stands originating from logging 80–150 years ago. Soils in all of the sites were sandy, acidic Spodosols on glacial till derived from the mica schist bedrock of Canaan Mountain.

The analysis of interspecific variation in light transmission presents a number of challenges when the species occur in

TABLE 1. Stand summaries for the six principal study sites

Dominant species*	Stand density (no./ha)	Stand basal area (m^2/ha)	Mean DBH (cm)	Mean height (m)	Relative density (%)	Relative basal area (%)
ACRU	738	27.6	19.8	18.7	88.6	79.1
ACSA	316	34.4	31.5	19.3	67.1	61.4
FAGR	665	38.3	26.0	18.3	44.3	31.2
FRAM	340	27.5	32.1	24.1	53.8	44.3
QURU	594	36.0	26.8	19.4	60.6	78.4
TSCA	570	55.4	29.9	17.9	46.0	49.6

NOTE: Density and basal area data are from either a 15 or 25 m radius plot centered in each stand. Stand density, stand basal area, mean DBH, and mean height are computed for individuals of all species ≥10 cm DBH. Relative density and basal area are given for the dominant species only.

*ACRU, red maple; ACSA, sugar maple; FAGR, beech; FRAM, white ash; QURU, red oak; TSCA, hemlock.

diverse, multispecies stands. Our principal approach was to use fisheye photography to allow analysis of light transmission through specified regions of the sky hemisphere. When combined with (*i*) maps of canopy tree distribution in the neighborhood around a photo point and (*ii*) estimates of the crown geometry of each tree in the neighborhood, this technique allows estimation (using procedures described below) of the effects of individual canopy trees on light regimes beneath them. However, several aspects of understory light regimes can not be estimated accurately from fish-eye photography. In particular, we used quantum sensors (Li-Cor Inc.) to estimate the importance of both sunflecks and beam enrichment (i.e., downward reflection of beam radiation). This effort required the use of stands dominated by a single target species, because of the 180° field of view of the sensors. Thus, for each of the six most common species, we selected a principal study site in which that species accounted for 44–88% of canopy tree density (Table 1). The sites were selected so that the dominant canopy species was also the dominant species in sapling size classes. While these six sites were each dominated by a single species, the total study area contained representatives of all nine of our target tree species. Each site was generally level (<5° slope) and 60–75 m in diameter, with no distinct gaps in the canopy. The locations of all canopy trees (stems ≥10 cm DBH) were mapped within either a 25 m radius (for the sugar maple, red maple, and hemlock stands) or a 15 m radius (for the beech, white ash, and red oak stands).

Canopy tree geometry

Regression equations predicting tree height and crown radius as a function of DBH, and crown depth as a function of height, were developed from measurements of crown geometry in 16–23 individuals of each of our nine study species. The sampled trees were randomly selected from two nearby mapped forest stands. Samples were stratified by size class to give a relatively uniform distribution of samples between 10 and 60 cm DBH. Crown depth was measured as the distance from the top of the tree to the lowest, nonepicormic foliage. The horizontally projected area of the crown was estimated as the area of an ellipse defined by measurement of the major and minor axes through the crown. The effective radius of the crown was computed as the radius of a circle with area equal to that of the ellipse. Height (H) of all species except hemlock and yellow birch was estimated from nonlinear least squares regression (SAS Institute Inc. 1987) on DBH using the equation: $H = a/(1 + b/\text{DBH})$, where a and b are species-specific constants. Over the size range from 10 to 60 cm, height of hemlock and yellow birch was better fit by a linear regression on DBH. Crown depth was estimated from linear least-squares regression on height. Crown radius was best predicted as a linear function of DBH (again using least-squares regression).

Understory PAR

PAR was measured at 10 locations in the understory of each of the six stands for a 5–10 day period in middle–late summer 1991 using quantum sensors (190SB sensors, Li-Cor Inc.) connected to a data logger (CR21X, Campbell Scientific Inc.). All sensors were leveled at a height of 1.0 ± 0.2 m. The sensors were placed 2–4 m to the north of the trunks of randomly chosen canopy trees of the dominant species in each stand. Sensors were separated from each other by a distance of at least 5 m. PAR measurements were made at 2-s intervals, and stored as half-hour minima, maxima, and means. The data logger also computed histograms of understory PAR in 100 $\mu mol \cdot m^{-2} \cdot s^{-1}$ classes each half hour. In operational terms, any instantaneous reading >100 $\mu mol \cdot m^{-2} \cdot s^{-1}$ was considered a sunfleck. This cutoff is high enough, given our estimated transmission coefficients for diffuse radiation in the different stands, to avoid counting bright diffuse light as a sunfleck; however, it is also low enough that most low-intensity sunflecks (due to penumbral effects, low sun angles, or haziness) would still be recognized. A full-sun sensor was monitored throughout the period in a nearby opening.

Canopy photography

Short-term PAR measurements are often poorly correlated with seasonal average light levels because of the geometry of both incident sunlight and canopy openings (Canham 1988; Rich et al. 1993). Computerized image analysis of hemispherical photos allows more robust estimates of long-term average light levels, as well as explicit analysis of the geometry of light penetration through forest canopies (Chazdon and Field 1987; Rich 1989; Canham et al. 1990). At each of the quantum sensor locations in the six main study sites, fish-eye photographs were taken at heights of 1, 2, 4, 6, and 7.5 m above the ground. In addition to the six intensively studied sites, secondary sites dominated by the remaining three species (yellow birch, black cherry, and white pine) were selected, and a set of 10 fish-eye photographs was taken beneath dominant canopy species of each of these three species, at 1-m height only. All photographs were taken with an Olympus 8-mm true fish-eye (equiangular) lens. The camera was leveled, with pointers in the image frame to indicate cardinal compass directions. Heights above 1 m were obtained by mounting the camera on a portable hydraulic hoist (Genie Inc.). All photographs were taken under overcast conditions, using fine-grained black and white film (TMAX-100 or TMAX-400, Kodak Inc.). All exposures were underexposed two f-stops to increase contrast between sky and foliage.

All of the fish-eye photographs were digitized at 512 × 512 resolution with a 256-level gray scale using commercial video image analysis hardware and software (C2, Olympus Corp.). The digitized images were then analyzed using software that computes a gap light index (GLI) using a modification of methods outlined in Canham (1988). In this study, the circular images produced by the fish-eye lens were divided into 480 regions representing equal areas of the sky hemisphere: 24 division of compass direction (azimuth) and 20 divisions of zenith angle,

each equal to 1/20 of the cos(zenith angle). The fraction of pixels in each grid cell occupied by unobscured sky was then multiplied by the fraction of total growing season radiation that originated from that region of the sky. Summing over the entire sky hemisphere gave GLI in units of percentage of full sun. Our method of calculating the distribution of open-sky radiation is described in Appendix 1.

Beam enrichment of understory light regimes

PAR in the forest understory consists primarily of beam and diffuse radiation that passes unhindered through openings ranging in size from sunflecks to large tree-fall gaps. We call this "gap" light, regardless of the size of the opening. In addition to gap light, understory PAR consists of (*i*) the relatively small amounts of diffuse and beam radiation that is transmitted through leaves and (*ii*) beam radiation that is successively reflected downward by foliage. This last component has been termed "beam enrichment" and has been shown to be a potentially important component of forest light regimes, particularly beneath closed canopies (Hutchison and Matt 1976). The GLI calculated from canopy photography estimates transmission of gap light only, not transmitted light or beam enrichment.

Quantum sensors are not capable of directly measuring beam enrichment. However, the magnitude of this component of understory radiation can be estimated using Hutchison and Matt's (1976) general approach. First, the average fraction of diffuse radiation that penetrates through the canopy (T_{diff}) (either directly through openings or transmitted through leaves) was calculated by comparing understory PAR data with the open site sensor for 30-min time periods when there was no direct sunlight in the open (i.e., when atmospheric transmission (K_T) was <0.4). Time periods when beam radiation was potentially present above the canopy, but during which individual understory sensors did not receive any significant amount of direct radiation through sunflecks were identified by selecting time periods when maximum understory light levels did not exceed 20% of the full sun maximum (although some of the radiation could have been low intensity penumbral radiation (e.g., Smith et al. 1989)). For each of these time periods, beam enrichment (BE) (as a fraction of understory PAR) at each sensor location was estimated as

$$[1] \quad BE = 1 - \frac{T_{diff} I_{diff}}{U_t}$$

where T_{diff} was the estimated average transmission coefficient for diffuse radiation for a given sensor, I_{diff} was the amount of diffuse radiation incident on the top of the canopy, and U_t was total understory PAR. The I_{diff} values were estimated from calculated K_T values using relationships given in Appendix 2. We did not attempt to estimate beam enrichment for time periods when understory sensors received direct beam radiation in the form of sunflecks because of the inability of quantum sensors to separate beam enrichment from sunflecks under those conditions.

Maximum likelihood estimation of species-specific extinction coefficients

Our core data sets consisted of maps of six stands showing the locations, diameters, and species of trees, and the digitized fish-eye photographs taken at 1 m height showing canopy openness in the sky hemisphere above each photo point. We estimated species-specific light extinction coefficients in four steps. First, we produced three-dimensional reconstructions of the stands by using the empirical allometric equations (relating DBH, height, crown depth, and crown diameter) to estimate the dimensions of a cylindrical crown for each mapped stem. Second, we divided each fish-eye photograph into 480 regions of equal area, using 24 horizontal partitions (spaced every 15° of azimuth) and 20 vertical partitions (spaced with equal cosine of zenith angle). We recorded the proportion of sky visible in each region (referred to below as "openness"). Third, consider the ray originating from the location of a fish-eye photograph and extending through the center of one of the photograph's 480 regions (along the region's mean azimuth angle and zenith angle with mean sine). Using the reconstructed three-dimensional map of the stand's canopy, we then recorded for each species: (*i*) the number of crowns intercepted by the ray (referred to as numbers of "hits") and (*ii*) the sum of the lengths of crown along the ray (referred to as "path lengths"). We repeated this procedure for each ray in each of the 90 photographs taken at 1-m height, but eliminated all rays that exited a stand below canopy height. This produced a data set with 2782 observations. Each observation contained a canopy openness, mean zenith and azimuth angles, and 18 numbers giving total number of hits and total crown lengths for each of the nine tree species.

Finally, we evaluated a series of regression equations (Appendix 3) to predict canopy openness, using variations on equations of the form

$$[2] \quad \text{Openness} = \exp\left(-\sum_{i=1}^{9} \lambda_i h_i\right)$$

where λ_i is a species-specific light extinction coefficient, and the meaning of h_i varies among the models. In the "absolute hits" model, h_i is the number of crowns of species i intercepted along a path. In the "relative hits" model, h_i is the proportion of crowns intercepted along the path that are of species i. In the "absolute path length" model, h_i is the total length traversed through crowns of species i along a given path, and in the "relative path length" model, h_i is the proportion of the length along a path that traverses through crowns of species i.

The hits models should be better approximations than the path length models when foliage is carried primarily at a crown's periphery. The path length models should be better when foliage is distributed evenly throughout the crown. The rationale behind the relative models is that our method of reconstructing the three-dimensional structure of stands does not account for the plasticity of crown shape. For example, the crowns of two mature trees with stems only 1 m apart may be virtually nonoverlapping in nature, but will overlap considerably in our reconstructions. Thus, the distribution of hits or path lengths used in the absolute hits and absolute path length models is undoubtedly too clumped. The relative hits and relative path length models represent the opposite extreme of zero overlap among crowns; the

TABLE 2. Shade tolerance and crown depth (as a percent of total tree height) for the nine study species

Species*	Sapling mortality (%/5 years)	Crown depth (%)	R^2
FAGR	2.6	50.3	0.40
TSCA	3.6	95.4	0.97
ACSA	14.8	66.9	0.81
BELU	23.5	71.2	0.56
PRSE	30.9	18.4	0.11†
PIST	31.7	47.2	0.55
ACRU	61.3	63.0	0.48
FRAM	72.9	39.4	0.43
QURU	80.8	47.0	0.42

NOTE: Shade tolerance was ranked by the predicted mortality for 2-cm DBH saplings (% mortality/5 years) at 0.5% full sun light level. Mortality rates were calculated from data on the relationships between light and radial growth (Pacala et al. 1993) and functional relationships between radial growth and sapling mortality (R.K. Kobe et al., see footnote 4). Crown depth was estimated from the slopes of linear regressions of crown depth as a function of tree height. Intercepts of the linear regressions for all nine species were not significantly different than zero. Also given are R^2 values for the regressions. The species are listed in order of decreasing shade tolerance.

*BELU, yellow birch; PRSE, black cherry; PIST, white pine. See Table 1 for the other species.

†$F = 3.65$, $p = 0.07$.

TABLE 3. Coefficients of regression equations for crown radius (m) as a linear function of DBH (m): radius = $a + b$ DBH and regression coefficients for tree height (H) as a function of DBH

	Crown radius				Tree height		
Species	a	b	R^2	Radius (m)*	a	b	Height (m)*
FAGR	2.32	8.26	0.79	6.45	32.9	17.3	24.4
TSCA	1.73	5.46	0.67	4.46	−0.729†	0.50	24.1
ACSA	1.65	6.37	0.74	4.84	44.0	31.9	26.9
BELU	1.24	6.44	0.35	4.46	6.83†	0.49	31.3
PRSE	0.39	10.60	0.79	5.69	37.4	19.4	26.9
PIST	0.69	7.11	0.56	4.25	68.1	70.6	28.2
ACRU	0.83	8.89	0.90	5.28	29.8	10.0	24.8
FRAM	0.66	7.84	0.68	4.58	34.9	9.8	29.1
QURU	1.71	7.92	0.79	5.67	37.6	18.0	27.6

NOTE: Height was a nonlinear function of DBH (m): $H = a/(1 + b/\text{DBH})$, for all species except yellow birch and hemlock. For these latter two species, height was a linear function of DBH: $H = a + b$ DBH, over the size range (10–60 cm DBH) used in this study. The tree species are listed in order of decreasing shade tolerance (see Tables 1 and 2).

*Crown radius and height of a 50 cm DBH tree.

†Linear regression of tree height on DBH, all others were nonlinear (see Methods).

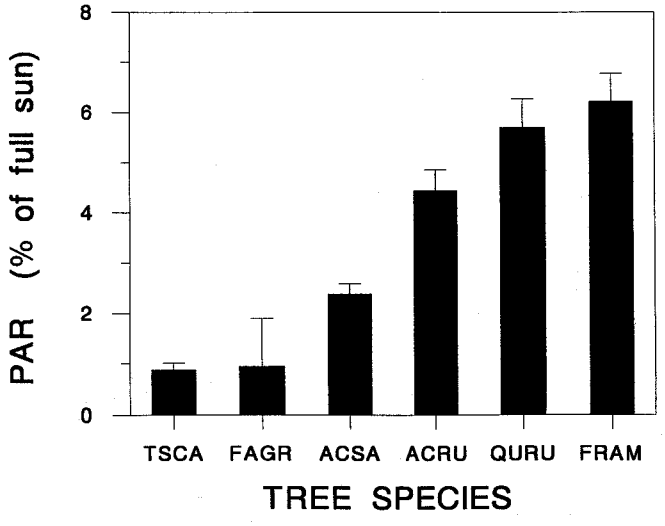

FIG. 1. Percent transmission of photosynthetically active radiation (PAR) through canopies dominated by six major tree species. Error bars are 1 SE; $n = 10$ sensor locations at 1 m height for each species (see Tables 1 and 2 for species).

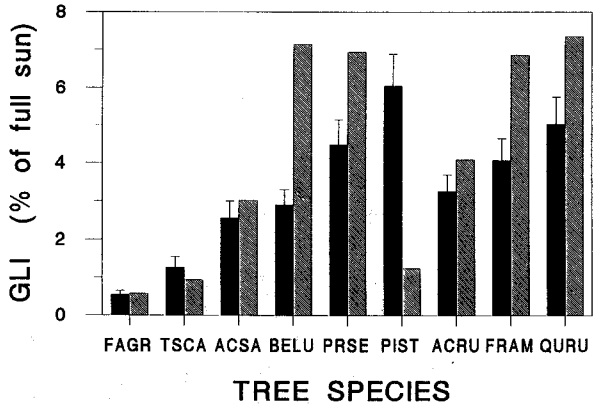

FIG. 2. Average gap light index (GLI) values at 1 m height beneath canopy trees of the nine study species (solid bars; error bars are 1 SE). Each species was sampled at 10 locations in a single stand in which the species was the single dominant species (see Tables 1 and 2 for species). Canopy tree species had a significant effect on average GLI ($F = 10.81$, df = 8, 81 $p < 0.0001$). The cross-hatched bars show the predicted GLI at ground level for a pure canopy of each species, using the light extinction coefficients estimated from the relative hits model (see Table 4).

overlap in our canopy reconstructions is "relativized away." We also developed canopy reconstructions by three-dimensional tessellation, which removes any overlap among crowns. However, fits of the absolute models using these were not as good as fits of the relative models using the simpler reconstructions relying on constant crown allometry.

In addition, we explored a variety of elaborations of this basic set of models. These included versions in which (*i*) shading was modified by zenith angle, (*ii*) there were separate extinction coefficients for adults and saplings, (*iii*) openness fell to a constant less than one even if no crowns were intercepted (the right hand sides were multiplied by a constant), and (*iv*) the exponents in the pure models were normalized in more complex ways than in the relative models (i.e., exponents were Michaelis–Menten functions that graded from absolute models at low shade to relative models at high shade). As shown below, the only successful modification was the inclusion of zenith angle as an independent variable in the relative models. Specifically, the exponent on the right hand side of both the relative hits and relative path length model was multiplied by the quantity: $1.0 - b(\Theta - 28.96)$, where Θ is zenith angle (zero at vertical), 28.96 is the mean zenith angle in our data set, and b was empirically derived using the maximum likelihood methods described in Appendix 3.

Results and discussion

Crown geometry

In general, the most shade-tolerant species had very deep crowns (50–95% of total tree height), while the least tolerant species had shallow crowns (18–63% of tree height) (Table 2). These differences in crown depth were more pronounced than differences in either crown radius or overall tree height (Tables 2 and 3). Crown radius was a linear function of stem diameter for all nine species (Table 3). Among the shade-tolerant species, beech trees had distinctively broad crowns (6.5 m radius for a 50 cm DBH tree), while hemlocks had relatively narrow crowns (4.5 m radius at 50 cm DBH) (Table 3). The rest of the species varied between 4.3

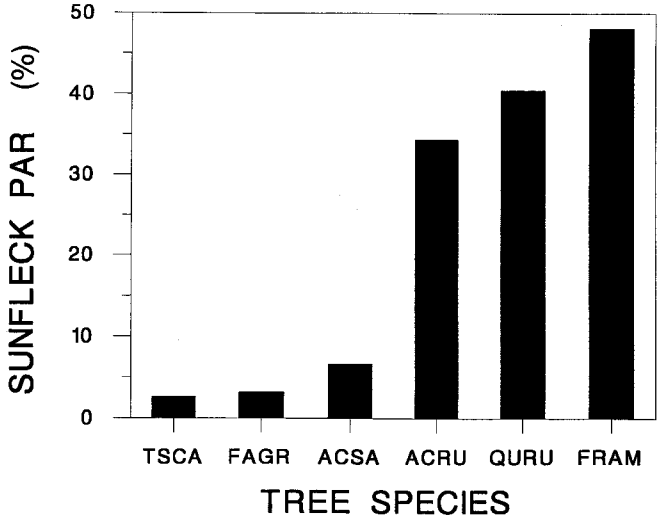

FIG. 3. Percentage of understory PAR received as sunflecks (i.e., at intensities >100 $\mu mol \cdot m^{-2} \cdot s^{-1}$) during the 5- to 10-day period of measurement in each of the six intensive study sites (see Table 1 for species).

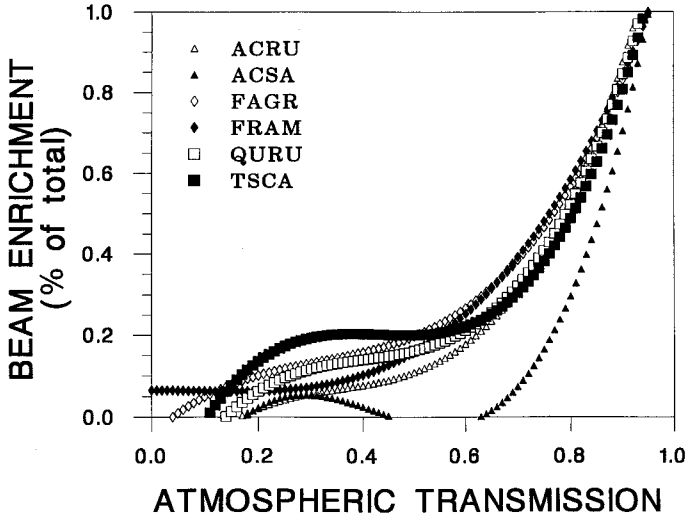

FIG. 5. Beam enrichment (as a percentage of instantaneous understory PAR) versus atmospheric transmission for the six intensive study sites (see Table 1 for species).

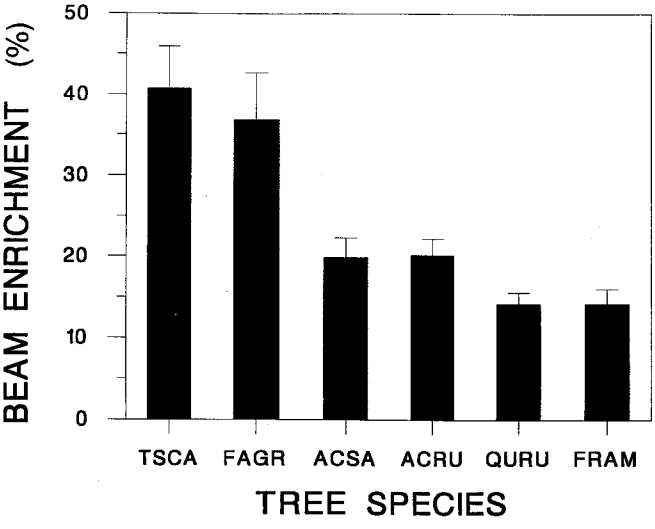

FIG. 4. Beam enrichment (as a percentage of total understory PAR) for the six intensive study sites (see Table 1 for species). Error bars are 1 SE of the mean for the 10 sensor locations in each site.

and 5.7 m radius at 50 cm DBH. Overall tree height was described well by a parabolic function of DBH for all species except yellow birch and hemlock (Table 3). Within the size range examined for this study (10–63 cm DBH), heights of these latter two species were a linear function of DBH. This reflects the short stature of understory and subcanopy hemlock and yellow birch trees relative to trees of similar DBH in the other species.

Stand-level variation in understory light regimes

Average transmission of integrated total PAR (measured with quantum sensors) by the six major tree species varied significantly ($F_{[5,54]} = 37.54$; $p < 0.0001$), and ranged from 0.9–6.2 % of full sun (Fig. 1). Light transmission was closely correlated with the shade tolerance of the dominant species in the stand, with the hemlock and beech stands casting the deepest shade (0.88 and 0.95%, respectively). The sugar maple and red maple stands cast intermediate levels of shade (2.4 and 4.4% of full sun, respectively), while the stands dominated by the two least tolerant species allowed the greatest light transmission (red oak, 5.7%; white ash, 6.2%).

GLI values, representing percent transmission integrated over the entire growing season, also varied significantly among species $F_{[8,81]} = 10.81$; $p < 0.0001$) (Fig. 2), and agreed closely with the integrated PAR data (Fig. 1). Average GLI values showed relatively continuous variation from the extremely low understory light levels of stands dominated by the shade-tolerant species (i.e., GLI = 0.54% for beech and 1.26% for hemlock), to the relatively high light levels of stands dominated by the shade-intolerant species (i.e. 5.0% for red oak) (Fig. 2). Our short-term measurements of PAR and growing season estimates of GLI are comparable with results of other studies of light transmission in closed forests of both temperate and tropical regions (e.g., March and Skeen 1976; Hutchinson and Matt 1977; Pearcy 1983; Chazdon and Fetcher 1984; Messier and Bellefleur 1988; Canham et al. 1990; Rich et al. 1993). Our results suggest that much of the variation in understory light levels observed in these studies is a predictable function of variation in canopy composition.

Our study sites were characterized by two distinctly different patterns of sunfleck frequency and importance. Stands dominated by the three early successional species (red oak, red maple, and white ash) all received relatively large proportions of understory PAR in the form of sunflecks, with locations beneath white ash trees receiving almost half (48.2%) of total PAR in the form of sunflecks (Fig. 3). These results are comparable with results from beneath closed canopies in a number of other temperate and tropical forests (e.g., Evans 1956; Bjorkman and Ludlow 1972; Pearcy 1983; Chazdon and Fetcher 1984; Chazdon 1988; Canham et al. 1990; Chazdon and Pearcy 1991). However, understory locations in stands dominated by the three most shade-tolerant species (hemlock, beech, and sugar maple), received only 2.6–6.6% of total understory PAR at intensities >100 $\mu mol \cdot m^{-2} \cdot s^{-1}$ (Fig. 3). It is likely that the very small size of canopy openings in these three stands resulted in a significant number of sunflecks that received only penumbral light (Smith et al. 1989) at intensities less than

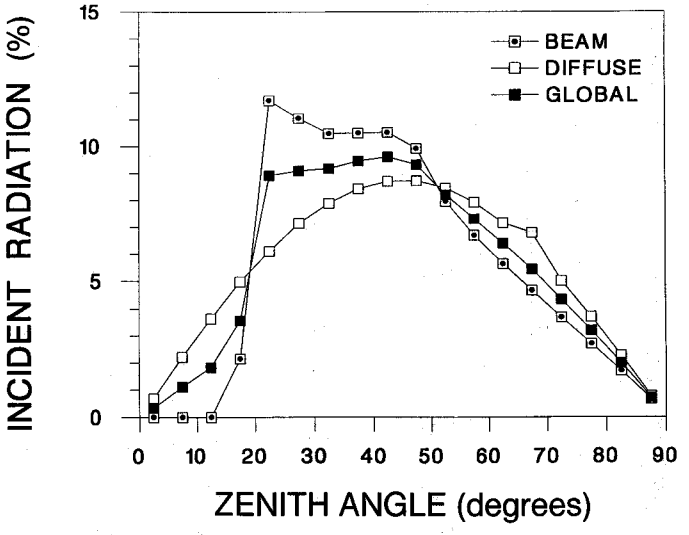

FIG. 6. Predicted amounts of direct beam, diffuse, and global radiation originating from 5° bands of the sky hemisphere. The calculations are for an open site at the latitude of our intensive study sites (42°N).

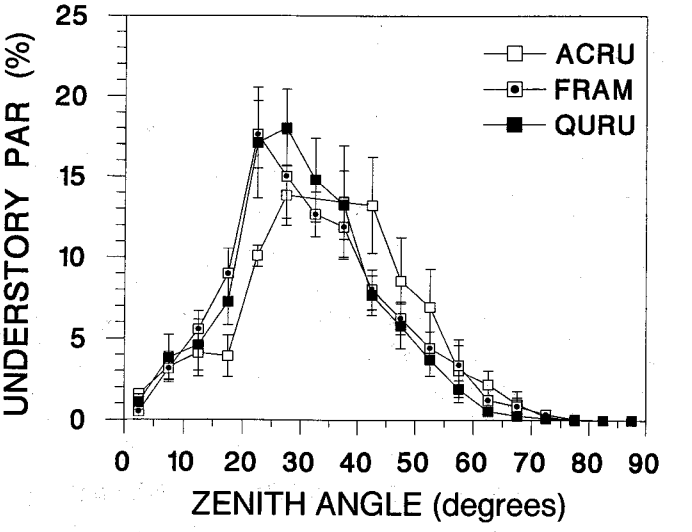

FIG. 7. Percentage of radiation in the understory beneath red maple (ACRU), white ash (FRAM), and red oak (QURU) canopies received from 5° bands of the sky hemisphere. The estimates are based on partitioning of GLI estimates from fish-eye photographs at 10 locations in each of the intensive study sites. Error bars are ±1 SE of the mean.

100 $\mu mol \cdot m^{-2} \cdot s^{-1}$, and that the total contribution of sunflecks was actually higher than indicated in Fig. 3. However, our results clearly indicate that the importance of sunflecks, and the overall degree of temporal variability in understory light regimes, will decline significantly during forest succession in these transition oak - northern hardwood forests.

While locations beneath beech and hemlock crowns received very little PAR in the form of sunflecks, we estimate that those locations received a significant fraction of PAR in the form of beam enrichment (37–41% of total understory PAR, respectively) (Fig. 4). Thus, GLI values determined from fish-eye photography will underestimate total PAR in stands dominated by the most shade-tolerant species. For all six stands, the importance of beam enrichment increased dramatically under clear skies (i.e., as K_T increased) (Fig. 5) (Hutchison and Matt 1976).

At the latitude of our study area (42°N), less than 7% of total growing season PAR originates from regions of the sky within 20° of the zenith (Fig. 6), largely because the sun never passes closer than within 19° of the zenith at this latitude. Instead, most radiation above the forest canopy originates from regions of the sky 20°–50° from the zenith, with amounts tapering off gradually towards the horizon (Fig. 6). Canopy openness is usually greatest directly overhead (data not presented, hemlock and beech are exceptions, with very low, uniform canopy openness, regardless of zenith angle). However, understory PAR in stands dominated by shade-intolerant species originates primarily from a narrow band of the sky between 20°–40° degrees from vertical (Fig. 7). Analysis of fish-eye photographs from a range of temperate and tropical forests revealed similar patterns (Canham et al. 1990). At angles closer to vertical, light transmission in both temperate and tropical forests is limited by the relatively low amounts of potential radiation (and the low relative area of sky within 20° of vertical). At angles closer to the horizon, light transmission is limited by the low openness of the canopy, presumably because of the long path length through tree crowns.

Average understory light levels (GLI) showed no significant variation with height within the range from 1–7.5 m

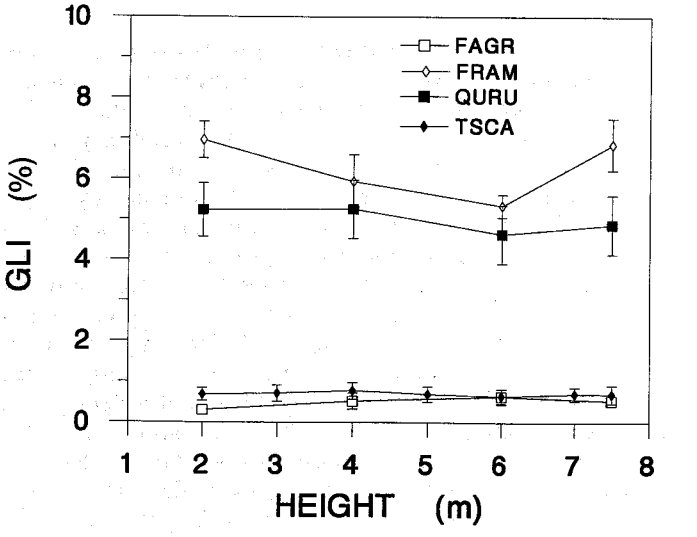

FIG. 8. Change in GLI with height for four representative species. Each species was sampled at 10 locations in a single stand in which the species was the single dominant species (see Table 1 for species). Error bars are ±1 SE of the mean.

above the ground for any of the six stands in which vertical gradients were measured (Fig. 8). Sapling densities were generally low in all of the sites except the beech-dominated stand, and very little canopy foliage occurred at heights <7.5 m except in the hemlock-dominated stand. Thus, there was little change in effective leaf area within the range of heights sampled in this study. In contrast, studies in temperate and tropical dry forests with more open canopies (Lin et al. 1992; Lerdau et al. 1992) have observed significant increases in light levels with height. In more mesic regions, we expect that GLI increases with height in stands with either a denser sapling layer or very numerous, small gaps.

Terborgh (1985), using a simple geometric model of light penetration, predicted distinct vertical strata in the understory with local maxima in average light levels and local minima in spatial variance. He proposed that this pattern

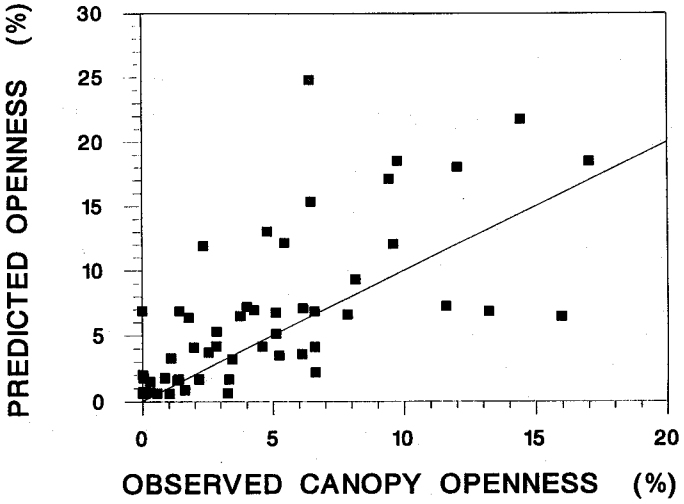

FIG. 9. Predicted canopy openness (using the relative hits model, Table 4) versus observed canopy openness for the 60 locations used to generate the calibration data set. Predicted and observed openness were calculated by summing over all of the path directions (zenith angle and azimuth) available for that location (given the position of the location within the mapped stand). The solid diagonal line is a 1:1 relationship.

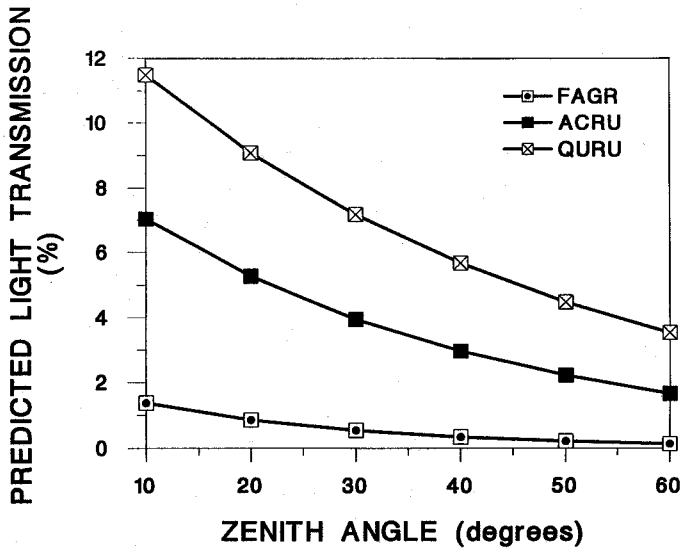

FIG. 10. Predicted relationships (using the relative hits model) between canopy openness and zenith angle for three representative species (see Table 1 for species).

could explain vertical stratification of understory tree species (Terborgh 1985). A subsequent, more detailed model (Pukkala et al. 1991) predicts more complex and less distinct vertical patterns in both the mean and horizontal variability, due to differences in latitude, crown shape, and the spatial distribution of trees; however, neither model provided any empirical validation of the predicted radiation regimes. Both models rely heavily on the occurrence of "crown shyness" gaps (i.e., zones of mutual avoidance by adjacent crowns) (Ng 1983). The Pukkala et al. (1991) model predicts that effects of crown shyness gaps will be distinct only within several meters of the bottoms of the crowns of canopy trees. It is possible that we would have observed a decrease in average GLI and an increase in spatial variability if we had been able to extend our sampling to heights of 15–20 m. The importance of crown shyness gaps is likely to vary significantly among canopy species, given the pronounced differences among our study species in crown depth (Table 2). The deep crowns of our late successional species do generally show zones of mutual avoidance (Kelty 1986), however these zones are quite convoluted, and do not provide a straight path for penetration of direct radiation. Thus, we suspect that if the patterns predicted by Terborgh (1985) and Pukkala et al. (1991) do exist, they will be limited to forests composed of shade-intolerant species with shallow crowns.

Species-specific light extinction coefficients

The light extinction model with the best fit to our data was the relative hits model (Fig. 9), in which canopy openness (percentage of sky visible) in any given portion of the sky was specified by eq. 2, where h_i is the proportion of intercepted trees represented by species i and λ_i is the species-specific extinction coefficient for a path made up entirely of that species. By relativizing the number of crowns intercepted along a path, this model removed the effect of zenith angle on the number of tree crowns through which light must pass. As a result, the model was significantly improved by multiplying the exponent by a coefficient (A) to incorporate the effect of zenith angle. Zenith angles in our data set ranged from 12°–43°, with a mean of 28.956°. We used a simple linear multiplier, with the form $A = 1.0 - b(\Theta - 28.956)$, where Θ was the zenith angle (in degrees), and b was the estimated slope of the multiplier (see Methods). For the relative hits model, $b = 0.009$ (95% confidence interval (CI) = 0.0077–0.0097). As a result, changing the zenith angle from 12° to 43° increased the extinction coefficient by 28% (Fig. 10).

The ranking of the extinction coefficients for the relative hits model (Table 4) corresponds very closely to the ranking of the GLIs for stands dominated by the respective species (Table 4, Fig. 2). The principal exceptions are white pine and yellow birch, for which our estimated extinction coefficients underestimate and overestimate, respectively, the observed light levels (Fig. 2). Our data set contained very few paths with either of these species, and we assume that the discrepancy reflects our limited data for these species. The other major difference between the understory light levels predicted from the calculated light extinction coefficients and GLI estimated directly from individual fish-eye photographs occurred in stands dominated by the early successional species. In these stands, simple GLI estimates calculated without regard to the specific species intercepting light in each section of the image resulted in lower estimates of light transmission than predicted by our more detailed analysis. This discrepancy occurred because the relatively low numbers of later successional species within these stands effectively reduced average light transmission, even at locations directly beneath the early successional species.

On the basis of the rankings presented in Table 4, we pooled the species into three groups: (*i*) hemlock and beech, (*ii*) sugar maple and red maple, and (*iii*) the remaining five species. Analysis of this pooled data set produced parameter estimates for the three groups that were not a significantly poorer fit to the data than the nine species model (likelihood for the pooled model, -4601.7 vs. -4595.4 for the full model, $p > 0.05$ df = 6). The estimated coefficients for the pooled model were 4.93 (95% CI = 4.76–5.09) for

TABLE 4. Maximum likelihood estimates of species-specific extinction coefficients with 95% confidence interval (CI) for three different models (see text for descriptions of the models)

	Absolute path length		Absolute no. of hits		Relative no. of hits	
Species	Estimate	95% CI	Estimate	95% CI	Estimate	95% CI
FAGR	0.298	0.144*	2.46	0.87*	5.17	4.77–5.47
TSCA	0.186	0.177–0.189	2.60	2.30–2.64	4.68	4.60–4.77
ACSA	0.142	0.136–0.144	0.88	0.79–0.89	3.50	3.11–3.51
BELU	0.209	—†	1.02	—†	2.64	0.02–4.31
PRSE	0.238	0.228–0.240	1.10	0.78–1.11	2.67	2.38–2.92
PIST	0.322	0.238–0.392	0.98	0.43–1.20	4.39	2.58–6.02
ACRU	0.134	0.133–0.135	0.87	0.79–0.88	3.20	3.10–3.22
FRAM	0.214	0.195–0.231	1.39	1.23–1.41	2.68	2.26–3.22
QURU	0.066	0.064–0.068	0.57	0.55–0.59	2.61	2.30–2.83
α	0.085	0.075–0.105	0.085	0.075–0.105	0.105	0.085–0.145
Likelihood		−4985		−4902		−4595

NOTE: Also listed are the estimated error term (α) and the overall likelihood for each model. Results are not presented for the relative path length model, which had the worst fit of the four basic models tested. The species are listed in order of decreasing shade tolerance (see Tables 1 and 2).

*Values are lower confidence limit only. The upper limit could not be calculated in these cases.

†Confidence interval could not be calculated in these cases.

TABLE 5. Predicted mortality rate (%/5 years) for saplings of each species under ambient light levels predicted for each canopy species (gap light index, GLI, using the relative hits model)

	Canopy species								
	FAGR	TSCA	ACSA	BELU	PRSE	PIST	ACRU	FRAM	QURU
GLI	0.6	0.9	3.0	2.9	6.9	6.1	4.1	6.9	7.4
Sapling species									
FAGR	2.6	2.5	2.2	2.2	2.1	2.1	2.2	2.1	2.1
TSCA	3.0	1.2	<0.1	<0.1	<0.1	<0.1	<0.1	<0.1	<0.1
ACSA	11.8	4.8	0.6	0.6	0.2	0.3	0.4	0.2	0.2
BELU	20.4	11.2	2.3	2.4	1.0	1.1	1.7	1.0	1.0
PRSE	25.0	8.5	0.1	0.1	<0.1	<0.1	<0.1	<0.1	<0.1
PIST	30.0	22.8	5.0	5.5	0.5	0.8	2.5	0.5	0.4
ACRU	56.0	34.4	2.7	3.1	0.1	0.2	0.1	0.1	0.1
FRAM	68.1	46.8	5.9	6.5	0.5	0.7	2.6	0.5	0.4
QURU	76.8	57.3	6.6	7.5	0.1	0.2	2.1	0.1	0.1

NOTE: Mortality rates were computed for saplings 2 cm DBH at the beginning of the 5-year period, using functional relationships between light and growth (Pacala et al. 1993) and relationships between growth and mortality given in R.K. Kobe et al. (see footnote 4). Because of the extremely large confidence intervals on our estimates of light extinction by yellow birch and white pine (Table 4), we have used the observed GLI data from fish-eye photographs (Fig. 2) for estimates of GLI in monospecific stands of those two species. Species are listed in order of decreasing shade tolerance (see Tables 1 and 2).

hemlock and beech, 3.20 (95% CI = 3.06–3.22) for the two maple species, and 2.81 (95% CI = 2.58–2.90) for the remaining five species. These extinction coefficients translate into predictions of 0.7, 4.1, and 6.0% canopy openness for pure stands of the three groups respectively. Pooling the two maple species in with the larger group of five species produced a significantly worse fit (likelihood = -4627, $p < 0.05$ df = 7).

The three other models (absolute hits, absolute path length, and relative path length) had significantly lower likelihoods than the relative hits model (Table 4). The estimated extinction coefficients for the absolute path length model suggest that the overall effect of a canopy tree species is not necessarily closely correlated with light extinction per unit length of path through the crown of a species (Table 4). For example, hemlock has only an intermediate extinction coefficient per unit length of crown; however, the very deep crowns of hemlocks (Table 2) produce the distinctively low light levels that characterize this species (Figs. 1 and 2). The two maple species also have low extinction coefficients per unit length of crown. However, again, their relatively deep crowns (Table 2) produce moderate to low light levels in the understory. In general, the fact that the hits models produced better fits than path length models agrees with results of studies that show uneven distribution of foliage within tree crowns (e.g., Kurachi et al. 1986). It is likely that the appropriateness of the models based on hits versus path length varies with the shade-tolerance of different species, with shade-tolerant species having more uniform distribution of foliage within a crown (path length model), while intolerant species have foliage distributed primarily at the periphery of the crown (hits model) (Horn 1971).

The zenith-angle multiplier for both of these models was not significantly different than zero, indicating that the decline in canopy openness with increasing zenith angle (Fig. 7) is caused simply by the increase in absolute path length as zenith angle increases, rather than a change in light transmission per unit path length due to the geometry of leaf inclination (Oker-Bloom and Kellomäki 1983).

The superior performance of the relative hits model is, in part, a reflection of the fact that the calibration data set consists of points near the forest floor, entirely beneath the crowns of canopy trees. For the purposes of modelling forest dynamics, the absolute hits model appears to be more appropriate because it can predict changes in light levels as saplings and subcanopy trees grow up through the canopy (Pacala et al. 1993).

Resource depletion versus resource tolerance

In related studies, we have quantified (*i*) sapling growth rates as a function of understory light regimes (Pacala et al. 1993) and (*ii*) sapling mortality as a function of growth rate (R.K. Kobe et al., to be published[4]). Results from those studies can be used to predict the relative tolerance of saplings to the shade cast by adults of the different species (Table 5). In all nine of the species, saplings have very low mortality rates in the shade cast by a canopy of conspecific adult trees (and any other species with higher light transmission), while only the three most shade-tolerant species (hemlock, beech, and sugar maple) have relatively low mortality rates (Table 5) under the very low light levels predicted for a monospecific stand of beech (the species with the lowest predicted canopy openness, based on the relative hits model (Table 4)).

Conclusions

Our study documents a very strong relationship between the shade tolerance of a species and its light extinction characteristics (Figs. 1 and 2, Tables 2 and 4). The results are clearly consistent with models of Horn (1971) and Connell and Slatyer (1977) that propose that secondary forest succession is driven by interspecific differences in resource uptake and tolerance. Our results suggest that the competitive dominants in the transition oak – northern hardwood forests of New England are the species that can reduce ambient levels of a critical resource (light) to levels that other tree species cannot tolerate (Tilman 1982) (Table 5). However, if more shade-tolerant competitors are absent from a stand, sapling mortality rates of even the intolerant species are low enough to allow successful development of advance regeneration in the shade cast by conspecific adults (Table 5; R.K. Kobe et al., see footnote 4).

It is clear from our results that crown geometry has an important effect on spatial variation in understory light regimes, and a simple but profound effect on forest succession. In general, the shade-tolerant species cast deep shade because of their deep crowns (Table 2), not because of high extinction coefficients per unit of crown depth (Table 4). This has important implications for the displacement of early successional species as a young stand is invaded by shade-tolerant species. The presence of a single hemlock tree in a red oak stand produces a zone of distinctively deep shade directly beneath the crown of the hemlock, largely because the foliage of the hemlock extends down close enough to the forest floor to block incident radiation at angles of 20°–40° from vertical. If hemlocks carried all of their foliage in a shallow crown 25–30 m above the forest floor, a single canopy tree would have only a modest effect on the understory because of the penetration of light from angles other than vertical. As more hemlocks invade the oak stand, their effect on understory light levels is amplified beyond the zones directly beneath their foliage, particularly in areas north of clumps of hemlock trees. In contrast, even though red oaks allow relatively high light transmission, a single red oak tree in a hemlock stand will have little effect on understory light levels, because the surrounding hemlocks will block the predominant incident radiation (at angles of 20°–50° from vertical). This pattern holds even in the extreme case of a single tree gap in a stand dominated by shade-tolerant species, where light levels suitable for growth of less tolerant species occur only in a small, transient zone under the canopy on the north edge of the gap (Canham 1988; Canham et al. 1990). Thus, while invasion of an early succesional stand by shade-tolerant trees is characterized by a positive feedback between resource depletion and the relative abundance of shade-tolerant species, the resulting late successional stand is relatively resistant to reinvasion by shade-intolerant species unless disturbances create large openings. While these patterns are most pronounced at high latitudes, the same general processes should occur in both temperate and tropical forests.

[4]R.K. Kobe, S.W. Pacala, J.A. Silander, and C.D. Canham. On the dimensionality of shade tolerance: sapling mortality as a function of growth history in a north temperate forest. To be published.

Acknowledgements

We thank Dawn Oswald, Coeli Hoover, Kai Ching Cha, and Eric Nelson for their assistance with field sampling. We also sincerely thank Star Childs and the Childs family, and the staff at Great Mountain Forest, for all of their support in making their field sites and excellent facilities available for this research, and the Bridgeport Hydraulic Company for making additional sites available for the research. Financial support was provided by the National Science Foundation (BSR 8918616) and the Mary Flagler Cary Charitable Trust. This study is a contribution to the program of the Institute of Ecosystem Studies.

Björkman, O., and Ludlow, M.M. 1972. Characterization of the light climate on the floor of a Queensland rainforest. Carnegie Inst. Washington Year Book, **71**: 85–94.

Botkin, D.B., Janak, J.F., and Wallis, J.R. 1972. Some ecological consequences of a computer model of forest growth. J. Ecol. **60**: 849–873.

Brokaw, N.V.L. 1985. Treefalls, regrowth, and community structure in tropical forests. *In* The ecology of natural disturbance and patch dynamics. *Edited by* S.T.A. Pickett and P.S. White. Academic Press, Orlando, Fla. pp. 53–68.

Canham, C.D. 1985. Suppression and release during canopy recruitment in *Acer saccharum*. Bull. Torrey Bot. Club, **112**: 134–145.

Canham, C.D. 1988. An index for understory light levels in and around canopy gaps. Ecology, **69**: 1634–1638.

Canham, C.D. 1990. Suppression and release during canopy recruitment in *Fagus grandifolia*. Bull. Torrey Bot. Club, **117**: 1–7.

Canham, C.D., Denslow, J.S., Platt, W.J., Runkle, J.R., Spies, T.A., and White, P.S. 1990. Light regimes beneath closed canopies and tree-fall gaps in temperate and tropical forests. Can. J. For. Res. **20**: 620–631.

Chazdon, R.L. 1988. Sunflecks and their importance to forest understory plants. Adv. Ecol. Res. **18**: 1–63.

Chazdon, R.L., and Fetcher, N. 1984. Photosynthetic light environments in a lowland tropical rainforest in Costa Rica. J. Ecol. **72**: 553–564.

Chazdon, R.L., and Field, C.B. 1987. Photographic estimation

of photosynthetically active radiation: evaluation of a computerized technique. Oecologia, **73**: 525–532.

Chazdon, R.L., and Pearcy, R.W. 1991. The importance of sunflecks for forest understory plants. BioScience, **41**: 760–766.

Clark, D.B., and Clark, D.A. 1991. The impact of physical damage on canopy tree regeneration in tropical rain forest. J. Ecol. **79**: 447–457.

Connell, J.H., and Slatyer, R.O. 1977. Mechanisms of succession in natural communities and their role in community stability and organization. Am. Nat. **111**: 1119–1144.

Denslow, J.S. 1980. Gap partitioning among tropical rainforest trees. Biotropica, **12**(Suppl.): 47–55.

Denslow, J.S. 1985. Disturbance-mediated coexistence of species. *In* The ecology of natural disturbance and patch dynamics. *Edited by* S.T.A. Pickett and P.S. White. Academic Press, Orlando, Fla. pp. 307–321.

Denslow, J.S. 1987. Tropical rainforest gaps and tree species diversity. Annu. Rev. Ecol. Syst. **18**: 431–451.

Edwards, A.W.F. 1972. Likelihood. Johns Hopkins University Press, Baltimore, Md.

Evans, G.C. 1956. An area survey method of investigating the distribution of light intensity in woodlands, with particular reference to sunflecks. J. Ecol. **44**: 391–428.

Gates, D.M. 1980. Biophysical ecology. Springer-Verlag, New York.

Goldberg, D.E. 1987. Neighborhood competition in an old-field plant community. Ecology, **68**: 1211–1223.

Grace, J.C. 1990. Modeling the interception of solar radiant energy and net photosynthesis. *In* Process modeling of forest growth responses to environmental stress. *Edited by* R.K. Dixon, R.S. Meldahl, G.A. Ruark, and W.G. Warren. Timber Press, Portland, Oreg. pp. 142–158.

Horn, H.S. 1971. The adaptive geometry of trees. Princeton University Press, Princeton, N.J. Monogr. Popul. Biol. 3.

Horn, H.S. 1974. The ecology of secondary succession. Annu. Rev. Ecol. Syst. **5**: 25–37.

Horn, H.S. 1975. Markovian properties of forest succession. *In* Ecology and evolution of communities. *Edited by* M.L. Cody and J.M. Diamond. Harvard University Press, Cambridge, Mass. pp. 196–211.

Horn, H.S. 1976. Succession. *In* Theoretical ecology. *Edited by* R.M. May. Blackwell, Oxford. pp. 187–204.

Hutchison, B.A., and Matt, D.R. 1976. Beam enrichment of diffuse radiation in a deciduous forest. Agric. Meteorol. **17**: 93–110.

Hutchison, B.A., and Matt, D.R. 1977. The annual cycle of solar radiation in a deciduous forest. Agric. Meteorol. **18**: 255–265.

Iqbal, M. 1983. An introduction to solar radiation. Academic Press, Orlando, Fla.

Kelty, M.J. 1986. Development patterns in two hemlock–hardwood stands in southern New England. Can. J. For. Res. **10**: 885–891.

Knapp, C.L., Stoffell, T.L., and Whitaker, S.D. 1980. Insolation data manual: long-term monthly averages of solar radiation, temperature, degree-days and global K_T for 248 National Weather Service stations. Solar Energy Research Institute, Washington, D.C.

Kurachi, N., Nagihara, A., and Hozumi, K. 1986. Distribution of leaf- and branch-biomass within a crown of Japanese larch and its relationship to primary production: analysis by sainome-cutting. *In* Crown and canopy structure in relation to productivity. *Edited by* T. Fujimori and D. Whitehead. Forestry and Forest Products Research Institute, Ibaraki, Japan. pp. 308–322.

Lerdau, M.T., Holbrook, N.M., Mooney, H.A., Rich, P.M., and Whitbeck, J.L. 1992. Seasonal patterns of acid fluctuations and resource storage in the arborescent cactus *Opuntia excelsa* in relation to light availability and size. Oecologia, **92**: 166–171.

Lin, T., Rich, P.M., Heisler, D.A., and Barnes, F.J. 1992. Influences of canopy geometry on near-ground solar radiation and water balances of pinyon–juniper and ponderosa pine woodlands. American Society for Photogrammetry and Remote Sensing, Falls Church, Va. Tech. Pap. pp. 285–294.

March, W.J., and Skeen, J.N. 1976. Global radiation beneath the canopy and in a clearing of a suburban hardwood forest. Agric. Meteorol. **16**: 321–327.

Messier, C., and Bellefleur, P. 1988. Light quantity and quality on the forest floor of pioneer and climax stages in a birch – beech – sugar maple stand. Can. J. For. Res. **18**: 615–622.

Metropolis, N., Rosenbluth, A.W., Rosenbluth, M.N., Teller, A.H., and Teller, E. 1953. Equation of state calculations by fast computing machines. J. Chem. Phys. **21**: 1087–1092.

Ng, F.S.P. 1983. Ecological principles of tropical lowland rainforest conservation. *In* Tropical rain forest: ecology and management. *Edited by* S.L. Sutton, T.C. Whitmore, and A.C. Chadwick. Blackwell, Oxford. pp. 359–375.

Norman, J.M. 1979. Modeling the complete crop canopy. *In* Modification of the aerial environment of plants. *Edited by* B.J. Barfield and J.F. Gerber. American Society of Agricultural Engineers, St. Joseph, Mich. pp. 249–277.

Norman, J.M., and Jarvis, P.G. 1975. Photosynthesis in Sitka spruce (*Picea sitchensis* [Bong.] Carr.). III. Measurements of canopy structure and interception of radiation. J. Appl. Ecol. **12**: 839–878.

Oker-Blom, P., and Kellomäki, S. 1982. Effect of angular distribution of foliage on light absorption and photosynthesis in the plant canopy: theoretical computations. Agric. Meteorol. **26**: 143–155.

Pacala, S.W., and Silander, J.A. 1985. Neighborhood models of plant population dynamics. I. Single-species models of annuals. Am. Nat. **125**: 385–411.

Pacala, S.W., and Silander, J.A. 1990. Field tests of neighborhood population dynamic models of two annual weed species. Ecol. Monogr. **60**: 113–134.

Pacala, S.W., Canham, C.D., and Silander, J.A., Jr. 1993. Forest models defined by field measurements. I. The design of a northeastern forest simulator. Can. J. For. Res. **23**: 1980–1988.

Pearcy, R.W. 1983. The light environment and growth of C_3 and C_4 species in the understory of a Hawaiian forest. Oecologia, **58**: 26–32.

Pearcy, R.W. 1987. Photosynthetic gas exchange responses of Australian tropical forest trees in canopy, gap and understory microenvironments. Funct. Ecol. **1**: 169–178.

Pukkala, T., Becker, P., Kuuluvainen, T., and Oker-Blom, P. 1991. Predicting spatial distribution of direct radiation below forest canopies. Agric. For. Meteorol. **55**: 295–307.

Rich, P.M. 1989. A manual for analysis of hemispherical canopy photography. Los Alamos National Laboratory, Los Alamos, N.M. Rep. LA-11733-M.

Rich, P.M., Clark, D.A., Clark, D.B., and Oberbauer, S.F. 1993. Long-term study of solar radiation regimes in a tropical wet forest using quantum sensors and hemispherical photography. Agric. For. Meteorol. In press.

Ross, J. 1981. The radiation regime and architecture of plant stands. W. Junk, The Hague.

Runkle, J.R. 1981. Gap regeneration in some old-growth mesic forests of eastern North America. Ecology, **62**: 1041–1051.

Runkle, J.R. 1985. Disturbance regimes in temperate forests. *In* The ecology of natural disturbance and patch dynamics. *Edited by* S.T.A. Pickett and P.S. White. Academic Press, Orlando, Fla. pp. 17–33.

SAS Institute Inc. 1987. SAS/STAT guide for personal computers, version 6 edition. Cary, N.C.

Shugart, H.H. 1984. A theory of forest dynamics. Springer-Verlag, New York.

Silander, J.A., and Pacala, S.W. 1985. Neighborhood predictors of plant performance. Oecologia, **66**: 256–263.

Smith, W.K., Knapp, A.K., and Reiners, W.A. 1989. Penumbral effects on sunlight penetration in plant communities. Ecology, **70**: 1603–1609.

Spitters, C.J.T., Toussaint, H.A.J.M., and Goudriaan, J. 1986. Separating the diffuse and direct component of global radiation and its implications for modeling canopy photosynthesis.

I. Components of incoming radiation. Agric. For. Meteorol. **38**: 217–229.

Szymura, J.M., and Barton, N.H. 1986. Genetic analysis of a hybrid zone between the fire-bellied toads near Cracow in southern Poland. Evolution, **40**: 1141–1159.

Terborgh, J. 1985. The vertical component of plant species diversity in temperate and tropical forests. Am. Nat. **126**: 760–776.

Tilman, D. 1982. Resource competition and community structure. Princeton University Press, Princeton, N.J.

Wang, H., and Baldocchi, D.D. 1989. A numerical model for simulating the radiation regimee within a deciduous forest canopy. Agric. For. Meteorol. **46**: 313–337.

Appendix 1: Calculation of the distribution of open-sky radiation

The distribution of open-sky radiation was calculated by combining estimates of diffuse and direct-beam radiation. Long-term measurements of diffuse radiation from quantum sensors mounted under a shadow band at the IES weather station in Millbrook, N.Y., indicate that roughly half of total growing season PAR is received as diffuse radiation (49.7% for the 1990 growing season). This agrees very closely with estimates of the regional importance of diffuse versus beam radiation calculated from data on atmospheric transmission (K_T) (Knapp et al. 1980). The more widely available K_T data indicate that our estimate that approximately 50% of total PAR in the open is received as diffuse radiation is appropriate for most of the northeastern United States in the summer (Knapp et al. 1980). Diffuse radiation can be very unevenly distributed (anisotropic) at any given time because of (*i*) variation in cloud conditions and (*ii*) diurnal variation in the position of the bright circumsolar region on clear days. However, we feel that the most reasonable assumption for the distribution of total diffuse radiation over a growing season is to assume that it is isotropic over the sky hemisphere. The contribution of any region of the sky to total diffuse radiation received by a horizontal surface, however, is still proportional to the cosine of the zenith angle for the region.

The distribution of open-sky, direct-beam radiation was estimated by calculating the position of the sun during the day at 5-min intervals throughout the growing season (May 1 – Sept. 30). The relative intensity of direct beam radiation (I_{beam}/I_o) on a horizontal surface at time t is given by $I_{beam}/I_o = E_o T^m \cos(\Theta_t)$ where Θ_t is the zenith angle of the sun, E_o is a daily correction factor for the eccentricity of the earth's orbit (Iqbal 1983), T is an average clear sky transmission coefficient (estimated as 0.65 for our region), and m is the path length through the atmosphere relative to a vertical path length ("air mass"). Air mass was calculated as $1/\cos(\Theta_t)$ for $\Theta < 65°$; with $m = 2.9$ for $65 \leq \Theta < 75°$; $m = 5.6$ for $75 \leq \Theta < 85°$; and $m = 10.39$ for $\Theta \geq 85°$, (Gates 1980). Beam intensity was assigned to a grid cell based on the zenith angle and azimuth of the sun at each time interval. Beam intensity in each grid cell was integrated over the growing season and then divided by the total sky intensity to calculate the percent of total beam radiation incident on a horizontal surface that originated from each of the 480 equal-area divisions of the sky hemisphere.

Appendix 2: Estimation of diffuse versus direct radiation from atmospheric transmission data

The fraction of incident radiation in the open received as diffuse (I_{diff}) versus direct beam radiation (I_{beam}) at any specific time is determined by the degree of scattering of beam radiation by the atmosphere. There is a well-known relationship between I_{beam} and the more readily calculated atmospheric transmission coefficient (K_T) (Spitters et al. 1986). The relationship is only approximate, because I_{beam} is most sensitive to scattering in the beam path, while K_T integrates transmission over the entire sky hemisphere. For this study, the relationship between I_{beam} and K_T was estimated from data for the 1990 growing season collected using quantum sensors and a shadow band at the IES weather station in Millbrook, N.Y. (approximately 50 km west of Great Mountain Forest). The relationship between I_{beam} and K_T was fit with a quadratic equation:

$$I_{beam} = -0.033\,01 + 0.210\,86\,K_T + 0.957\,97\,K_T^2, \qquad R^2 = 0.83$$

At K_T values below 0.4, beam radiation is negligible or absent. I_{beam} increases rapidly as K_T rises from 0.4 to 0.9, and then reaches an upper limit set by the scattering of solar radiation by a clear sky. I_{beam} is also influenced by the zenith angle of the sun, particularly at very large zenith angles (i.e., near the horizon), where the path length for solar radiation through the atmosphere begins to increase rapidly, leading to increased scattering of beam radiation even under clear skies. However, our data show this to be a minor effect except very early or late on clear days.

Appendix 3: The likelihood model

To develop a regression method for estimating light extinction coefficients, we first grouped the data into categories with similar values of the independent variables (hits, path lengths, relative hits, or relative path lengths) within each category. In categories corresponding to heavy shade (many hits, long path lengths, etc.), the distribution of openness had a low mean and decreased monotonically, with an openness of zero being most common and an openness of one being least common. In categories of light shade (few hits, etc.), the distribution had a higher mean and was U-shaped (local maxima at zero and one, with lower values in between). Apparently, canopy openness becomes progressively more patchy as shade decreases.

These observations suggested that the regression method be developed around a β-distribution. The β-probability density function may be written as

$$[A1] \quad \beta(y \mid a, M) = \frac{y^{a-1}(1-y)^{a(1/M-1)-1}}{W(a, M)}$$

where

$$W(a, M) = \int_0^1 v^{a-1}(1-v)^{a(1/M-1)-1}dv, \qquad 0 < y < 1,\ 0 < M < 1,\ 0 < a$$

where y is openness, M is mean openness, and a is a parameter controlling the shape of the distribution. If $a < 1$ (as it is shown to be below in this application), then, like the observed distributions of openness, $\beta(y|a, M)$ is monotonically decreasing at low means and U-shaped at high means.

However, there is a difficulty in basing a likelihood regression model of canopy openness on the β-density. Observed values of openness are commonly either zero or one, and the β-density asymptotes to infinity at these values. Thus, the likelihood given by [A1] is undefined for an observed value of zero. For this reason, we discretized the β-density as follows.

Suppose that we divide the interval from zero to one into $1/\Delta y$ segments of length Δy. The first segment contains values of openness from zero to Δy, the second contains values: $\Delta y < y \leq 2\Delta y$, the third contains values: $2\Delta y < y \leq 3\Delta y$, and so on. Using [A1], the probability that a randomly chosen openness, is contained in the kth segment ($P(k|a, M)$ is defined to be

$$[A2] \quad P(k|a, M) = \int_{(k-1)\Delta y}^{k\Delta y} \beta(y|a, M)dy$$

Now consider an observed openness, y_i, with its associated vector of independent variables, x_i. This vector would include the numbers of hits for each species in the absolute hits model, the path length for each species in the absolute path length model, and so on. Also, let the expected mean for the ith openness be a function of the independent variables, $M(x_i|q)$, where q is the vector of parameters that we wish to estimate (such as the λ_is). Thus, $M()$ would be equal to the right hand side of eq. 2, with h_i being the number of hits of species i if we wished to estimate the extinction coefficients in the absolute hits model.

Finally, suppose that $r(y_i/\Delta y)$ is the smallest integer greater than or equal to $y_i/\Delta y$. Then, using [A2], the *likelihood* of y_i is: $P(r(y_i/\Delta y)|a, M(x_i|q))$, and the log-likelihood of the entire set of N observed opennesses is

$$[A3] \quad l(q, a) = \sum_{i=1}^{N} \ln\left(P\left(r\left(\frac{y_i}{\Delta y}\right)|a, M(x_i|q)\right)\right)$$

We employed a simulated annealing technique based on the Metropolis algorithm (Metropolis et al. 1953; Szymura and Barton 1986), to find the values of q and a that maximize [A3], and obtained confidence limits for each estimate by inverting the likelihood-ratio test (Edwards 1972). Plots of residuals, observed against expected means, and observed against expected variances indicate that the method lacks debilitating systematic bias (see Results).

To produce all estimates described in the Results, we discretized the β-density into 300 segments ($\Delta y = 1/300$). We obtained identical estimates with 100 and 1000 segments in exploratory analyses. Estimates varied with the number of segments if there were fewer than 50. Also, to save computational time, we produced estimates and confidence limits of the shape-controlling parameter, a, only to an accuracy of 0.005. In preliminary analyses, accuracies of 0.005 and 0.001 led to identical estimates of the remaining parameters.